

15 Oct 2002

Photoreflectance Spectroscopy of Strained (In)GaAsN/GaAs Multiple Quantum Wells

J. B. Heroux

Xiaodong Yang

Missouri University of Science and Technology, yangxia@mst.edu

W. I. Wang

Follow this and additional works at: https://scholarsmine.mst.edu/mec_aereng_facwork



Part of the [Aerospace Engineering Commons](#), and the [Mechanical Engineering Commons](#)

Recommended Citation

J. B. Heroux et al., "Photoreflectance Spectroscopy of Strained (In)GaAsN/GaAs Multiple Quantum Wells," *Journal of Applied Physics*, vol. 92, no. 8, pp. 4361-4366, American Institute of Physics (AIP), Oct 2002. The definitive version is available at <https://doi.org/10.1063/1.1507817>

This Article - Journal is brought to you for free and open access by Scholars' Mine. It has been accepted for inclusion in Mechanical and Aerospace Engineering Faculty Research & Creative Works by an authorized administrator of Scholars' Mine. This work is protected by U. S. Copyright Law. Unauthorized use including reproduction for redistribution requires the permission of the copyright holder. For more information, please contact scholarsmine@mst.edu.

Photoreflectance spectroscopy of strained (In)GaAsN/GaAs multiple quantum wells

J. B. Héroux,^{a)} X. Yang, and W. I. Wang

Department of Electrical Engineering, Columbia University, New York, New York 10027

(Received 10 June 2002; accepted for publication 23 July 2002)

The effect of a variation of the indium and nitrogen concentrations in $\text{In}_x\text{Ga}_{1-x}\text{As}_{1-y}\text{N}_y/\text{GaAs}$ multiquantum wells grown by molecular beam epitaxy is studied systematically by room temperature photoreflectance spectroscopy. The band gap redshift caused by a nitrogen fraction of 1.5% decreases by as much as 30% as the indium fraction increases from 0% to 20%. A moderate increase of electron effective mass ($\Delta m_e \sim 0.03 m_0$) is found in all samples containing nitrogen ($y \geq 1\%$). In compressively strained quantum wells, the energy separation between the first confined heavy and light hole energy levels decreases in a regular manner as the nitrogen fraction increases from 0% to 1.7%, suggesting that the modification of the valence bands due to nitrogen incorporation can be explained by the strain variation. © 2002 American Institute of Physics. [DOI: 10.1063/1.1507817]

INTRODUCTION

The compound $\text{In}_x\text{Ga}_{1-x}\text{As}_{1-y}\text{N}_y$ (Ref. 1) has attracted much attention recently due to its potential for the fabrication of GaAs-based optoelectronic devices operating in the near infrared.² When a small fraction of nitrogen atoms is incorporated into (In)GaAs, both the band gap and the free lattice parameter are decreased. Therefore, for quantum wells grown on a GaAs substrate, either the compressive strain is lessened in high indium content layers or a tensile strain is created in low indium content layers. For a certain ratio $x \approx 3y$, the new quaternary compound can be grown lattice matched to the substrate.

The incorporation of nitrogen leads to the formation of an impurity level located about 200 meV above the conduction band minimum in GaAs.³ The strong redshift of the band gap observed experimentally has been explained by a repulsion between this energetic level and the Γ conduction band, while the valence band is assumed to be nearly unperturbed.^{4–6} Band mixing with the L and X bands is also believed to be important.^{7–10} A shift of the conduction band minimum independent of any interaction with other electronic states may be another factor contributing to the band gap decrease.⁸ Localized energy levels due to nitrogen pairs or other atomic clusters are also formed around the conduction band either in the gap or the continuum^{11,12} and some of the unusual physical properties of the compound could be due to a hybridization of the conduction band minimum with these localized states.^{9,10}

To date, much of the fundamental work done theoretically and experimentally on diluted nitrides has been focused either on the GaAsN ternary compound (see, e.g., Refs. 5,7,9,10,13–19) or on InGaAsN layers lattice matched to GaAs (see, e.g., Refs. 4,6,8,20), even though some of the most promising results for laser diodes have been obtained

using highly strained, high indium content InGaAsN quantum wells.²¹ Although the use of a ternary or lattice-matched quaternary compound as a starting point for fundamental studies of bulk layers may simplify result analysis, the choice of the most simple structure may be different for the optical characterization of heterostructures when the goal is to determine how the band gap, effective masses, and the band alignment are fundamentally modified by nitrogen incorporation. The valence band offset of GaAsN/GaAs heterostructures is small, and this has led to much uncertainty in determining whether the fundamental band alignment of this material system is type I^{13,14} or type II.^{15,16} It has caused confusion in the assignment of the conduction band confined energy levels in quantum wells, which has led in turn to very large discrepancies in the reported values of the conduction band effective mass. In a recent paper, Zhang *et al.*¹³ obtained m_e^* values as high as $0.55 m_0$ by assuming that optical transitions involving the second confined conduction band energy level could not be observed in GaAsN/GaAs structures since only one confined valence band energy level was formed. Experimenting with similar structures, Wu *et al.*¹⁷ obtained, on the other hand, values around $0.1 m_0$, five times lower, by assuming that transitions involving the second electronic energy level could indeed be observed. Another drawback of GaAsN/GaAs structures is that for a very small nitrogen fraction (below, say, 1% for a well width around 100 Å or less) the conduction band offset becomes so small that transitions involving excited electronic states, essential for the accurate determination of many physical parameters, are not observed.

Using instead the well understood, widely studied InGaAs/GaAs material system as a starting point to study the effect of nitrogen incorporation experimentally has several advantages. For a relatively high indium fraction, say, around 15%, the valence and conduction band offsets are non-negligible regardless of the nitrogen concentration so that a number of optical transitions can be observed, tracked, and

^{a)} Author to whom correspondence should be addressed; electronic mail: jbh14@columbia.edu

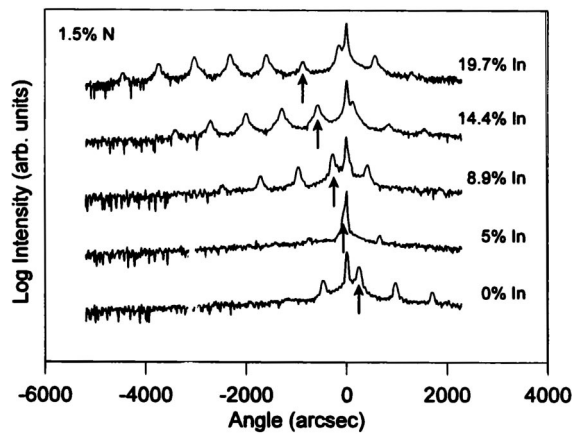


FIG. 1. X-ray diffraction spectra of $\text{In}_x\text{Ga}_{1-x}\text{As}_{0.985}\text{N}_{0.015}/\text{GaAs}$ ($82 \text{ \AA}/200 \text{ \AA}$) multiquantum well structures. Arrows indicate the zero order satellite peaks. The 5% In sample is nearly lattice matched so that satellite peaks are almost invisible.

unambiguously identified. Moreover, if a small nitrogen fraction is added, the wells are still compressively strained. Therefore, the fundamental transition should necessarily involve heavy holes and the energy separation between confined levels involving the heavy and light hole bands should be larger than in a lattice-matched or tensile strained structure, making it easier experimentally to resolve the optical transitions and quantify the effect of strain variation. Finally, the quantum well width can be determined *a priori* using a nitrogen-free structure as a reference, simplifying the analysis. In this work, we chose the latter approach and studied systematically and independently the effect of a variation of both the indium and nitrogen concentrations in $\text{InGaAsN}/\text{GaAs}$ multiquantum wells (MQWs) in order to better understand the physical properties of this material system.

EXPERIMENTAL RESULTS AND CALCULATIONS

Two series of $\text{In}_x\text{Ga}_{1-x}\text{As}_{1-y}\text{N}_y/\text{GaAs}$ MQW samples in which only the indium (first series) or nitrogen (second series) fraction was varied were grown by molecular beam epitaxy using a plasma rf nitrogen source (SVT Inc.). All samples were nonintentionally doped, and had ten periods with 200 \AA thick barriers and a 500 \AA GaAs cap. Structural characterization was done by x-ray diffraction (XRD) in the 400 and 511 orientations. Optical characterization was done at room temperature by photoreflectance (PR) using a Spex 500 M spectrometer and a photodiode pulsed at 1 kHz emitting at a wavelength of 670 nm with an output power of 1 mW. A third derivative functional form was used to simulate the PR spectra and obtain the transition energies.

Figure 1 shows XRD spectra of the first series of samples, in which the indium fraction was varied. The parameters of the second sample in the series (14.4% In) were estimated by growing and characterizing by XRD and low temperature transmittance a nominally identical, nitrogen-free structure and assuming that the difference in average strain between the two samples—found from the position of the satellite peak maxima—was entirely due to nitrogen incorporation, i.e., that the well width and indium fraction

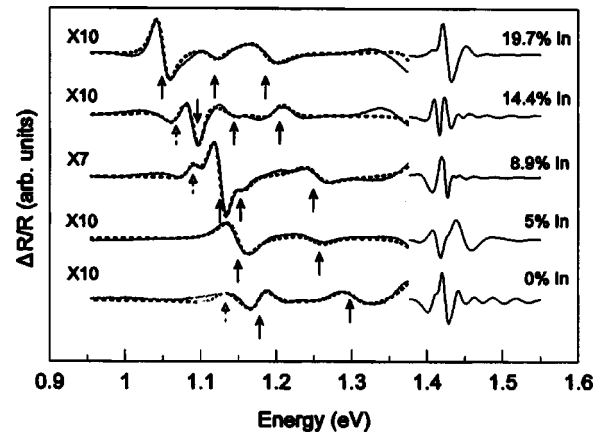


FIG. 2. Room temperature photoreflectance spectra of the samples described in Fig. 1. Arrows indicate the energy transitions obtained using third derivative functional form curve fits, shown by dashed lines. Dashed arrows indicate defect-related transitions.

were unchanged. A well width of 82 \AA was found with a nitrogen fraction of 1.5%. Vegard's law is expected to be accurate in this nitrogen composition range²² so that systematic errors are avoided. The indium fraction of the remaining samples in the series was then estimated by measuring their average strain and assuming that the variation from one sample to another was entirely due to the different indium composition, i.e., that neither the well width nor the nitrogen fraction varied. The average strain of the GaAsN/GaAs sample was such that the same nitrogen composition, 1.5%, was found by assuming a constant well width of 82 \AA , as expected. The arrows in Fig. 1 indicate the zero order satellite peaks. The 19.7%, 14.4%, and 8.9% indium samples are compressively strained, while the 5% and 0% indium samples are nearly lattice matched and tensile strained, respectively.

Figure 2 shows the photoreflectance spectra obtained for this series of samples. The three distinct optical transitions marked by arrows visible for the 19.7%, 14.4%, and 8.9% In samples are associated with the first heavy hole to first electron (hh1-e1), first light hole to first electron (lh1-e1) and second heavy hole to second electron (hh2-e2) transitions, respectively, with increasing energy. Hetterich *et al.*²³ performed polarization-dependent photoluminescence excitation measurements on highly strained InGaAsN single quantum wells, confirming the nature of the optical transitions observed. Other groups^{24,25} also observed these transitions for this material system and assigned them in a similar manner.

As the indium composition decreases, the two lower energy transitions involving the h1 and l1 energy levels get closer to each other and cannot be resolved for the 5% and 0% In samples. Because of the small difference in indium concentration among the samples, the evolution of the higher transition can, however, still be tracked and positively associated with the e2 energy level for the 5% and 0% In samples. The intensity ratio of the first (fundamental) to the highest (e2 associated) transition decreases with the indium fraction and becomes closer to unity for the GaAsN/GaAs sample. Extra features located below the fundamental transition can be seen on the 14.4%, 8.9%, and 0% In samples and

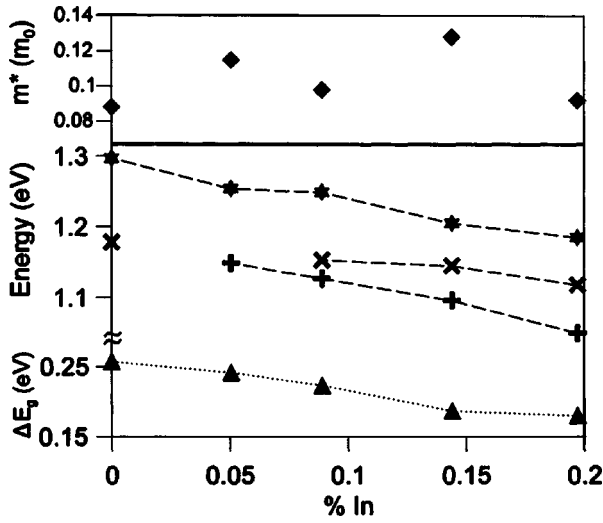


FIG. 3. Data points in the middle of the figure indicate the energy levels found experimentally and associated with the 1hh-1e (+), 1lh-1e (×), and 2hh-2e (★) energy levels, respectively. For the 5% and 0% In samples, the exact nature of the valence energy levels involved is unclear. The dashed lines are an aid to the eye. Triangles (▲) in the lower part of the figure show the redshift of the band gap due to nitrogen incorporation calculated from the transitions observed experimentally. Diamonds (◆) in the upper part show the electron effective masses also calculated from the experimental data. Exciton binding energies were neglected in the calculations for simplicity but this does not affect the conclusions reached.

are believed to be defect-related; Shanabrook *et al.*²⁶ observed similar features in GaAs/AlGaAs quantum wells. Oscillations above the GaAs-related transitions are also visible and are due to the finite thickness of the cap layer and the high potential barrier at the surface.²⁷

The middle part of Fig. 3 shows how the observed optical transitions evolve and can be tracked as the indium fraction decreases from 19.7% to 0%. Rather than use a predefined model to perform a single fit of all observed transitions, results were simulated independently for each sample to avoid any bias in the interpretation; a single band envelope function formalism was used to find the bulk unstrained band gap and conduction band effective mass in the well. These two parameters were adjusted until an agreement better than 1 meV was reached for the fundamental (*e1* associated) and the highest confined (*e2* associated) optical transitions. By assuming that the unstrained valence band offset was unchanged by nitrogen incorporation and modifying the splitting of the heavy and light hole valence bands to take into account the strain variation in the wells due to nitrogen, an agreement within 6 meV was obtained for the observed lh1-*e1* transitions. The unstrained valence band offset ΔE_{v_u} was calculated by assuming, based on the work of Joyce *et al.*,²⁸ a strained InGaAs/GaAs band offset ratio $Q_c = \Delta E_c / \Delta E_{v_{hh}} = 0.65$ for $x \geq 8\%$ and 0.57 for $x \approx 5\%$. ΔE_{v_u} varied from 28 meV (19.7% In) to 0 meV (0% In). The biaxial strain was calculated based on the usual Pikus-Bir Hamiltonian,²⁹ with the energy shifts due to hydrostatic δE_H and shear δE_S strain components expressed as

$$\begin{aligned} \delta E_H &= 2a(1 - C_{12}/C_{11})\varepsilon, \\ \delta E_S &= -2b(1 + 2C_{12}/C_{11})\varepsilon, \end{aligned} \quad (1)$$

were ε is the strain tensor in the plane of the interfaces, C_{11} and C_{12} are elastic stiffness constants, and a and b are the hydrostatic and shear deformation potentials, respectively. The hydrostatic component was applied to the conduction band, while the shear component corresponds to the splitting between the heavy hole and light hole bands. Since the nitrogen fraction is small and is expected to affect mostly the conduction band, the elastic constants, deformation potentials, and hole effective masses were assumed not to be modified by nitrogen incorporation and standard values³⁰ were used for all these parameters.

The lower part of Fig. 3 shows the calculated energy difference between the unstrained band gap in the well of the samples of this series and the one that would be obtained using a standard expression³⁰ for a similar compound without nitrogen. The band gap redshift due to the constant nitrogen fraction is lowered by as much as 30% as the indium fraction increases. This can be explained using a two level model, according to which the band gap of the quaternary material is given by⁴

$$\begin{aligned} E_g(\text{In}_x\text{Ga}_{1-x}\text{As}_{1-y}\text{N}_y) \\ = \frac{E_M(x) + E_N - \sqrt{[E_M(x) - E_N]^2 + 4V_{NM}^2(x,y)}}{2}, \end{aligned} \quad (2)$$

where E_N is the nitrogen impurity level located above the conduction band minimum of a nitrogen-free alloy E_M and $V_{NM} = C_{NM}\sqrt{y}$ (Ref. 31) is the quantum interaction between the two levels. It can be assumed that the position of the impurity level E_N relative to the vacuum level does not change much as indium is incorporated^{10,32} but the extended level E_M moves downward. The energy difference between the E_M and E_N levels increasing with the indium fraction, the quantum coupling is reduced so that the band gap redshift due to a constant nitrogen fraction is lowered for a higher indium fraction. Assuming typical values $E_N = 1.65$ eV, $E_M = E_g(\text{InGaAs})$, and $C_{NM} = 2.7$ eV with $y = 0.015$, a reduction of the band gap redshift due to nitrogen of 31% is found if x increases from 0 to 0.2, in good agreement with the experimental data. The results recently published by Serries *et al.*³³ for samples with a higher indium composition grown on an InP substrate also corroborate our own.

The upper part of Fig. 3 shows the electron effective masses determined as described above. The values, although slightly scattered due to the fact that individual fits were performed for each sample, are consistently larger than the ones that would be obtained for nitrogen-free samples. No regular dependence of the effective mass with the indium fraction can be observed within experimental precision. Using a two level model,⁶ we expect this dependence to be small and values comparable to the ones shown here are predicted. Kent and Zunger^{9,10} proposed that above a small critical nitrogen concentration y_c , the interaction of the extended conduction band with localized nitrogen pairs and other higher order cluster states in GaAsN could explain the increased electronic effective mass. If so, the addition of indium shifting down the conduction band does not seem to significantly modify this interaction.

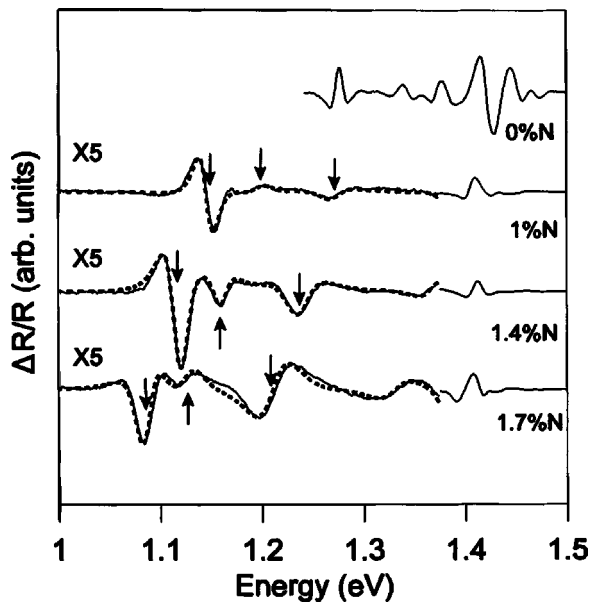


FIG. 4. Room temperature photoreflectance spectra of a series of $\text{In}_{0.14}\text{Ga}_{0.86}\text{As}_{1-y}\text{N}_y/\text{GaAs}$ ($86 \text{ \AA}/200 \text{ \AA}$) multiquantum well samples. Arrows indicate the energy transitions obtained using third derivative functional form fits, shown by dashed lines.

Figure 4 shows photoreflectance spectra obtained for the second series of multiquantum well samples in which the nitrogen fraction was varied and the wells are compressively strained. The well width and indium fraction of the nitrogen-free sample were found to be 86 \AA and 14.3% , respectively, and were assumed to remain constant in all samples so that the nitrogen concentration could be estimated from the average strain measured by XRD. The identification of the first heavy hole to the first conduction band ($1\text{hh}-1e$), first light hole to first conduction band ($1\text{lh}-1e$) and second heavy hole to second conduction band ($2\text{hh}-2e$) transitions is straightforward in all samples, and was also independently verified by low temperature transmittance measurements presented elsewhere.³⁴

A plot of the energy difference between the $1\text{hh}-1e$ and $1\text{lh}-1e$ transitions obtained experimentally, shown by the data points in the lower part of Fig. 5, provides a simple way to probe the valence band in these structures since the same conduction band energy level is involved in both transitions. The $\text{hh}-\text{lh}$ splitting predominantly depends on two factors: the shear deformation potential b and the valence band offset. The solid lines in the figure show a calculation of the $\text{hh}-\text{lh}$ energy splitting for the quantum wells investigated here assuming a shear deformation potential unchanged by nitrogen incorporation ($b = -1.97 \text{ eV}$) with constant unstrained band offsets corresponding to strained $\text{In}_{0.14}\text{Ga}_{0.86}\text{As}/\text{GaAs}$ band offset ratios $Q_c = 0.7$ (Ref. 30; $\Delta E_{v_u} = 13 \text{ meV}$, lower solid curve) and $Q_c = 0.65$ (Ref. 28; $\Delta E_{v_u} = 20 \text{ meV}$, upper solid curve). In a recent article Zhang *et al.*³⁵ proposed that the shear deformation potential could be increased in bulk GaAsN samples to an absolute value higher than 3 eV . The dashed lines in the figure therefore show the same calculation (i.e., same ΔE_{v_u} values) performed with $b = -3 \text{ eV}$. Clearly, in our case a better agree-

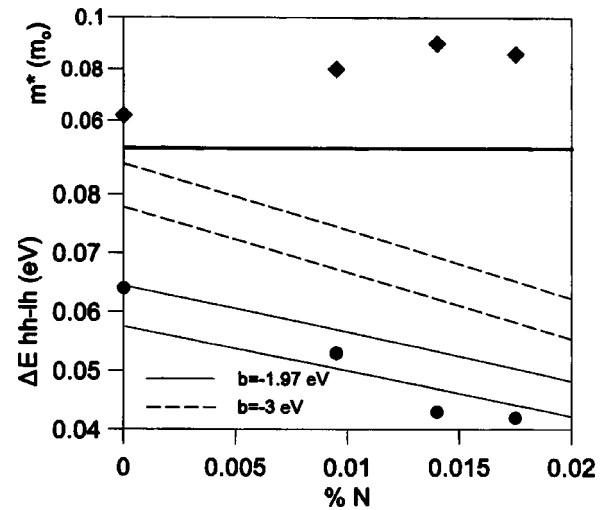


FIG. 5. Circles (\bullet) indicate the experimental values of the energy difference between the first two optical transitions shown in Fig. 4, associated with the first heavy and light hole energy levels, respectively. Diamonds (\blacklozenge) indicate the electron effective mass calculated from the transitions observed experimentally. Solid and dashed lines show theoretical calculations of the $\text{hh}-\text{lh}$ splitting assuming shear deformation potentials $b = -1.97 \text{ eV}$ and $b = -3 \text{ eV}$, respectively. An exciton binding energy of 8 meV was assumed for the transitions involving the heavy hole band only (see Ref. 30).

ment is obtained assuming a constant (i.e., lower absolute value) shear deformation potential. The upper part of Fig. 5 shows again that nitrogen incorporation results in a moderate increase of the conduction band effective mass (see next section).

DISCUSSION

Figure 6 illustrates the postulated valence band structure used for the calculations presented in the previous section, based on the assumption of a constant unstrained valence

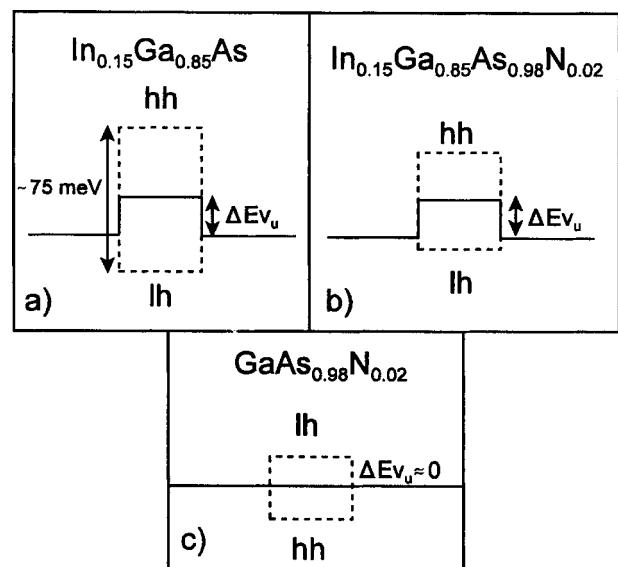


FIG. 6. (a) Valence band configuration of a compressively strained $\text{In}_{0.15}\text{Ga}_{0.85}\text{As}/\text{GaAs}$ quantum well. (b) Effect of the incorporation of a nitrogen fraction around 2% . The unstrained band offset ΔE_{v_u} remains constant in both cases. (c) GaAsN/GaAs valence band configuration. The offset is due to the tensile strain and $\Delta E_{v_u} \approx 0$.

band offset. In high indium content quantum wells, nitrogen incorporation reduces the compressive strain, and hence the heavy hole–light hole band splitting, as shown in (a) and (b). The heavy hole band alignment is type I in lattice-matched or compressively strained wells. For an indium fraction around 15% and a nitrogen fraction lower than 2%, the decrease of the hh–lh band splitting is not large enough to modify the type of the light hole band alignment and it is expected to remain type II. In GaAsN/GaAs quantum wells, the valence band offset is due to the tensile strain, with type I and type II alignments for the light and heavy hole bands, respectively.

While a small shift (upward or downward) of the unstrained valence band alignment due to nitrogen incorporation cannot be ruled out, there are many reasons to believe that such a shift, if it occurs, is not large. First and most importantly, nearly all theoretical papers published to date (see, e.g., Refs. 8–10 and 31) and predict the absence of any significant intrinsic perturbation of the valence band due to nitrogen. Second, the regular decrease of the hh–lh splitting observed in Fig. 5 as the nitrogen fraction increases strongly suggests that the modification of the valence band is due to strain variation. While these experimental values of the hh–lh splitting could also be reproduced with a calculation assuming a decrease of the unstrained band offset in conjunction with a relatively large increase of the absolute value of the shear deformation potential (e.g., $\Delta E_{v_u} \rightarrow 0$ and $b \rightarrow -3$ eV), the hypothesis of a valence band modified entirely by strain is a much more simple—hence more attractive—explanation in better agreement with theoretical articles. Third, in Fig. 2 the hh–lh splitting is clearly observed in quantum wells with a high indium fraction but not in the 5% and 0% In spectra, strongly suggesting that the valence band offset becomes small as the indium fraction decreases. Fourth, as noted in the Introduction, there are important discrepancies in the literature concerning the type of band alignment found experimentally for the GaAsN/GaAs material system, so that the valence band offset of this heterostructure must be in reality very small.

The simple model schematically described in Fig. 6 can also account for the observation of an optical transition involving the $e2$ energy level even in the absence of a second confined light hole state in GaAsN/GaAs quantum wells. The light hole valence band well is very shallow and should have a single confined energy level located only a few meV below the GaAs barrier. Its parity may be not well defined due to interface roughness so that a lh1– $e2$ transition could be observed. Furthermore, there may be more than one heavy hole state confined in the GaAs layers acting as wide wells, and interwell coupling could occur due to the narrowness of the GaAsN barriers so that a hh2– $e2$ transition may be observed. Since the two types of transitions cannot be resolved experimentally, the confined light hole and heavy hole levels might be so close to each other to be considered for practical purposes merged—as for tensile strained quantum wells with other material systems³⁶—and the valence band assumed to be nearly flat. If one considers for simplicity a one-dimensional structure with a completely flat valence band and a conduction band well having two confined states with

wave functions of even and odd parities, clearly the usual interband transition parity rule would not apply³⁷ and transitions involving both electronic states would be allowed, as we observe experimentally.

Based on these considerations, we propose that Wu *et al.*¹⁷ used the correct optical transition assignment for their calculation of the electron effective mass in GaAsN/GaAs structures but that the very high values exceeding the GaAs heavy hole effective mass and the sharp decrease as the nitrogen fraction increases above 1% reported by Zhang *et al.*¹³ are due to an incorrect assignment of the second observed transition with the third conduction band confined energy level. If we exclude these last results, there is an overall agreement in the literature that the incorporation of a nitrogen concentration around 1% in nonintentionally doped structures leads to an increase of the electron effective mass to a value in the range 0.08–0.12 m_0 and that the dependence on the indium concentration is relatively weak; the values obtained in this work are in reasonably good agreement with those reported by Wu *et al.*¹⁷ ($m_e^* \approx 0.11 m_0$ with 1.2%–2.8% N, 0% In), Hai *et al.*¹⁸ ($m_e^* \approx 0.12$ – $0.19 m_0$ with 1.2%–2% N, 0% In), Hetterich *et al.*²³ ($\Delta m_e^* \approx 0.03 m_0$ with 1.5% N, 38% In) and Pan *et al.*²⁴ ($m_e^* \approx 0.075$ – $0.095 m_0$ with 0.35%–1% N, 30% In).

CONCLUSION

It should be stressed that the goal of this article is not to present the most precise and definite values of the effective mass or other parameters of this material system for device design. Rather, we sought to: positively identify the optical transitions observed experimentally for this material system; observe specific trends in the properties of the material system as the atomic fractions vary; and explain some of the discrepancies found in the literature. An optical transition associated with the second confined conduction band energy level is observed in structures with and without indium so that the increase of the conduction band effective mass due to a 1% nitrogen fraction is around $\Delta m_e \sim 0.03 m_0$. The band gap redshift due to nitrogen is found to decrease as the indium composition increases. In compressively strained quantum wells the regular decrease of the energy difference between the heavy and light hole energy levels as the nitrogen fraction increases can be explained by the strain variation.

¹M. Kondow, T. Kitatani, S. Nakatsuka, M.C. Larson, K. Nakahara, Y. Yazawa, M. Okai, and K. Uomi, *IEEE J. Sel. Top. Quantum Electron.* **3**, 719 (1997).

²See, e.g., J.B. Héroux, X. Yang, and W.I. Wang, *Appl. Phys. Lett.* **75**, 2716 (1999); Y.S. Jalili, P.N. Stavrinou, J.S. Roberts, and G. Parry, *Electron. Lett.* **38**, 343 (2002).

³D.J. Wolford, J.A. Bradley, K. Fry, and J. Thompson, in *Physics of Semiconductors*, edited by D.J. Chadi and W.A. Harrison (Springer, New York, 1984), p.627.

⁴W. Shan, W. Walukiewicz, J.W. Ager III, E.E. Haller, J.F. Geisz, D.J. Friedman, J.M. Olson, and S.R. Kurtz, *Phys. Rev. Lett.* **82**, 1221 (1999).

⁵J.D. Perkins, Am. Mascarenhas, Y. Zhang, J.F. Geisz, D.J. Friedman, J.M. Olson, and S. R. Kurtz, *Phys. Rev. Lett.* **82**, 3312 (1999).

⁶C. Skierbiszewski, *et al.*, *Appl. Phys. Lett.* **76**, 2409 (2000).

⁷T. Mattila, S.H. Wei, and A. Zunger, *Phys. Rev. B* **60**, R11245 (1999).

⁸A. Al-Yacoub and L. Bellaiche, *Phys. Rev. B* **62**, 10847 (2000).

⁹P.R.C. Kent and A. Zunger, *Phys. Rev. Lett.* **86**, 2613 (2001).

¹⁰P.R.C. Kent and A. Zunger, *Phys. Rev. B* **64**, 115208 (2001).

- ¹¹X. Liu, M.E. Pistol, L. Samuelson, S. Schwetlick, and W. Seifert, *Appl. Phys. Lett.* **56**, 1451 (1990).
- ¹²X. Liu, M.E. Pistol, and L. Samuelson, *Phys. Rev. B* **42**, 7504 (1990).
- ¹³Y. Zhang, A. Mascarenhas, H.P. Xin, and C.W. Tu, *Phys. Rev. B* **61**, 7479 (2000).
- ¹⁴I.A. Buyanova, G. Pozina, P.H. Hai, W.M. Chen, H.P. Xin, and C.W. Tu, *Phys. Rev. B* **63**, 033303 (2000).
- ¹⁵T. Kitatani, M. Kondow, T. Kikawa, Y. Yazawa, M. Okai, and K. Uomi, *Jpn. J. Appl. Phys., Part 1* **38**, 5003 (1999).
- ¹⁶B.Q. Sun, D.S. Jiang, Z. Pan, L.H. Li, and R.H. Wu, *J. Cryst. Growth* **227-228**, 501 (2001).
- ¹⁷J. Wu, W. Shan, W. Walukiewicz, K.M. Yu, J.W. Ager III, E.E. Haller, H.P. Xin, and C.W. Tu, *Phys. Rev. B* **64**, 085320 (2001).
- ¹⁸P.N. Hai, W.M. Chen, I.A. Buyanova, H.P. Xin, and C.W. Tu, *Appl. Phys. Lett.* **77**, 1843 (2000).
- ¹⁹P.J. Klar, H. Gruning, W. Heimbrodt, J. Koch, F. Hohnsdorf, W. Stolz, P.M.A. Vicente, and J. Carnassel, *Appl. Phys. Lett.* **76**, 3439 (2000).
- ²⁰P. Perlin, P. Wisniewski, C. Skierbiszewski, T. Suski, E. Kaminska, S.G. Subramanya, E.R. Weber, D.E. Mars, and W. Walukiewicz, *Appl. Phys. Lett.* **76**, 1279 (2000); E.D. Jones, N.A. Modine, A.A. Allerman, S.R. Kurtz, A.F. Wright, S.R. Tozer, and X. Wei, *Phys. Rev. B* **60**, 4430 (1999).
- ²¹See, e.g., G. Steinle, H. Riechert, and A. Yu. Egorov, *Electron. Lett.* **37**, 93 (2001); N. Jikutani, S. Sato, T. Takahashi, A. Itoh, M. Kaminishi, and S. Satoh, *Jpn. J. Appl. Phys., Part 1* **41**, 1164 (2002).
- ²²W.J. Fan, S.F. Yoon, T.K. Ng, S.Z. Wang, W.K. Loke, R. Liu, and A. Wee, *Appl. Phys. Lett.* **80**, 4136 (2002).
- ²³M. Hetterich, M.D. Dawson, A. Yu. Egorov, D. Bernklau, and H. Riechert, *Appl. Phys. Lett.* **76**, 1030 (2000).
- ²⁴Z. Pan, L.H. Li, Y.W. Lin, B.Q. Sun, D.S. Jiang, and W.K. Ge, *Appl. Phys. Lett.* **78**, 2217 (2001).
- ²⁵G. Sek, K. Ryczko, J. Misiewicz, M. Fischer, M. Reinhardt, and A. Forchel, *Thin Solid Films* **380**, 240 (2000).
- ²⁶B.V. Shanabrook, O.J. Glembocki, and W.T. Beard, *Phys. Rev. B* **35**, 2540 (1987).
- ²⁷S. Fafard, E. Fortin, and A.P. Roth, *Phys. Rev. B* **45**, 13769 (1992).
- ²⁸M.J. Joyce, M.J. Johnson, M. Gal, and B.F. Usher, *Phys. Rev. B* **38**, 10978 (1988); M.J. Joyce, Z.Y. Xu, and M. Gal, *ibid.* **44**, 3144 (1991).
- ²⁹G.E. Pikus and G.L. Bir, *Sov. Phys. Solid State* **1**, 136 (1959); **1**, 1502 (1960).
- ³⁰G. Ji, D. Huang, U.K. Reddy, T.S. Henderson, R. Houdré, and H. Morkoç, *J. Appl. Phys.* **62**, 3366 (1987); G. Ji, U.K. Reddy, D. Huang, T.S. Henderson, and H. Morkoç, *Superlattices Microstruct.* **3**, 539 (1987).
- ³¹A. Lindsay and E.P. O'Reilly, *Solid State Commun.* **112**, 443 (1999).
- ³²J.M. Langer and H. Heinrich, *Phys. Rev. B* **55**, 1414 (1983).
- ³³D. Serries, T. Geppert, P. Ganser, M. Maier, K. Kohler, N. Herres, and J. Wagner, *Appl. Phys. Lett.* **80**, 2448 (2002).
- ³⁴J.B. Héroux, X. Yang, and W.I. Wang, *J. Vac. Sci. Technol. B* **20**, 1154 (2002).
- ³⁵Y. Zhang, A. Mascarenhas, H.P. Xin, and C.W. Tu, *Phys. Rev. B* **61**, 4433 (2000).
- ³⁶A. Baliga, D. Trivedi, and N.G. Anderson, *Phys. Rev. B* **49**, 10402 (1994).
- ³⁷G. Bastard, *Wave Mechanics Applied to Semiconductors* (Hastled, New York, 1988).